Visualization of NMDA receptor-dependent AMPA receptor synaptic plasticity *in vivo*

Yong Zhang[1,2,*], **Robert H. Cudmore**[1,*], **Da-Ting Lin**[1,2,†], **David J. Linden**[1], and **Richard L. Huganir**[1,2]

[1]Solomon H. Snyder Department of Neuroscience, Johns Hopkins University School of Medicine, Baltimore, Maryland 21205, U.S.A

[2]Howard Hughes Medical Institute, Johns Hopkins University School of Medicine, Baltimore, Maryland 21205, U.S.A

Abstract

Regulation of AMPA receptor (AMPAR) membrane trafficking plays a critical role in synaptic plasticity and learning and memory. However, how AMPAR trafficking occurs *in vivo* remains elusive. Using *in vivo* two-photon microscopy in the mouse somatosensory barrel cortex, we found that acute whisker stimulation leads to a significant increase in the surface expression of the AMPAR GluA1 subunit (sGluA1) in both spines and dendritic shafts and small increases in spine size. Interestingly, initial spine properties bias spine changes following whisker stimulation. Changes in spine sGluA1 are positively correlated with changes in spine size and dendritic shaft sGluA1 following whisker stimulation. The increase in spine sGluA1 evoked by whisker stimulation is NMDA receptor dependent and long lasting, similar to major forms of synaptic plasticity in the brain. These results reveal experience dependent AMPAR trafficking in real time and characterize, *in vivo*, a major form of synaptic plasticity in the brain.

AMPARs mediate the majority of fast excitatory synaptic transmission in the central nervous system, and, as such, are critical targets for experience-dependent regulation of information processing and storage in the brain. Long-term potentiation (LTP) and long-term depression (LTD) of excitatory synaptic transmission in the central nervous system are major forms of synaptic plasticity that are thought to be critical for experience dependent modification of brain function such as learning and memory. AMPAR trafficking to and from synapses is a highly dynamic process, which mediates certain forms of LTP and LTD;

increases in AMPAR function at synapses result in LTP, whereas removal of synaptic AMPARs leads to LTD[1-3]. Thus, understanding the temporal and spatial dynamics and molecular processes governing experience-dependent AMPAR plasticity *in vivo* is crucial to understand how experience shapes brain function and behavior in health and disease.

Previous studies have shown that chronic sensory deprivation resulting from whisker trimming regulates spine turnover *in vivo*[4,5]. However, due to the lack of functional synaptic markers these studies fail to address the effect of sensory manipulation on relative synaptic strength or AMPAR trafficking in preexisting stable spines. Manipulation of chronic whisker experience through stimulation or trimming has also been shown to regulate AMPAR content and subunit composition in the barrel cortex in *ex vivo* slices[6,7], but the *ex vivo* nature of these studies preclude real-time acute or longitudinal analysis of AMPAR dynamics. Here, we transfected layer 2/3 pyramidal neurons in mouse barrel cortex with the AMPAR GluA1 subunit tagged with a pH-sensitive form of GFP (Super Ecliptic pHluorin, SEP), the AMPAR GluA2 subunit tagged with myc, and a morphological marker dsRed2 using *in utero* electroporation[8] and then monitored AMPAR dynamics through a cranial window in anesthetized animals using two-photon microscopy. Our data show that acute whisker stimulation leads to a significant increase in spine sGluA1 and shaft sGluA1 in a subpopulation of dendrites. Whisker stimulation evoked changes in spine sGluA1 are positively correlated with changes in spine size and shaft sGluA1. Moreover, acute whisker stimulation induced increases in spine sGluA1 is NMDA receptor dependent and long lasting, suggesting acute whisker stimulation might lead to a LTP like phenomenon *in vivo*. Our study indicates that measuring surface postsynaptic receptor dynamics is a new way of monitoring and dissecting the mechanisms of synaptic plasticity in real time *in vivo*.

Results

In vivo imaging of AMPARs in layer 2/3 neurons in the barrel cortex

The primary somatosensory cortex has an exquisite somatotopic map in which each individual whisker is represented as a discrete anatomical unit, the "barrel", allowing precise delineation of functional organization, development, and plasticity[9]. To monitor AMPAR dynamics and spine turnover in the barrel cortex we transfected layer 2/3 neurons with SEP-GluA1, myc-GluA2 and dsRed2 by in utero electroporation on E15 embryos. We used low concentrations of DNA for electroporation in order to minimize the degree of AMPAR overexpression and to sparsely label a small population of neurons. Immunostaining of GluA1 in brain slices of electroporated animals show that the transfected neurons have only modest overexpression of GluA1 (Supplementary Fig. 1). We then made a cranial window over the barrel cortex in 10 week old mice that had previously undergone neuronal transfection via *in utero* electroporation[10]. Following a 2–3 week recovery period to allow inflammation to subside (Supplementary Fig. 2), individual barrel columns were mapped using intrinsic optical signal (IOS) imaging (Fig. 1a, b) and *in vivo* two-photon images of apical dendrites from layer 2/3 neurons both within and outside the mapped barrel columns were acquired in anesthetized animals[10-12]. Transfected neurons had high expression of SEP-GluA1 in synaptic spines throughout the dendritic arbor with a relatively lower expression within dendritic shafts (Fig. 1c, movies S1 and S2). The basal expression of SEP-

GluA1 in spines *in vivo* had a wide distribution and was correlated with spine size (Fig. 1d), consistent with previous findings that the number of postsynaptic AMPARs is strongly correlated with spine size[13,14] and most likely a determinant of synaptic strength[15]. Interestingly, we observed dramatic differences in SEP-GluA1 expression at spines along the same dendrite within a few microns of each other (Fig. 1c). In extreme cases some spines express high levels of SEP-GluA1 while neighboring spines have barely detectable levels.

To determine the basal stability of SEP-GluA1 distribution over time; we imaged neurons repeatedly in the absence of sensory manipulation. We were able to detect stable expression of both dsRed2 and SEP-GluA1 at individual spines in the cortex for over one month and the relative expression of SEP-GluA1 at specific synapses could also be maintained over this period (Fig. 2a). Since AMPARs have a metabolic half-life of 30–40 hours[16] the AMPARs at the end of the month are different proteins than those observed at the beginning of the imaging period. This indicates that GluA1 is targeted to specific spines within a dendrite and there is an inherent mechanism to maintain the relative level of surface AMPARs along dendrites across many rounds of receptor turnover.

Acute whisker stimulation leads to an increase in spine and shaft sGluA1

To examine whether acute sensory stimulation regulates AMPAR surface expression in the barrel cortex we deflected a single whisker at 10 Hz for 1 hour and images were taken immediately before whisker stimulation and following whisker stimulation at 1, 2, and 3 hours within the corresponding barrel column of the deflected whisker (Fig. 2b). Control animals were imaged at the time-points with no whisker stimulation. Studies in brain slices have shown that chronic sensory experience can drive GluA1 into synapses between layer 4 and layer 2/3 neurons through an LTP-like process[7,17,18]. We monitored surface AMPAR dynamics *in vivo*, and found that acute whisker stimulation leads to a $\sim 30\%$ average increase in spine sGluA1 on preexisting spines on dendrites within the stimulated barrel (Figs. 2b, 3b, Supplementary Fig. 3c, d). In contrast, we did not observe a significant change in average spine sGluA1 from dendrites of distant unstimulated barrels or in control unstimulated animals (Fig. 3e). This increase in spine sGluA1 following whisker stimulation was rapid, occurring within the first hour after stimulation and persisted for at least 3 hours. To further characterize the change in spine sGluA1 following whisker stimulation, we grouped spines based on their percent change at 1 hour into three categories: same, up, and down. Using the SD of the percent change at 1 hour in control animals as a threshold ($\pm$ 30%) we grouped spines as: same ($> 70\%$ and $< 130\%$), up ($\geq 130\%$), and down ($\leq 70\%$). One hour following the onset of whisker stimulation, there is a dramatic increase in the population of spines in the up category (35% vs. 10%), a significant decrease in the population of spines in the same category (55% vs. 74%), and no change in the population of spines in the down category (10% vs. 16%) (Fig. 3d). We also investigated the dynamics of sGluA1 in the dendritic shaft underlying each spine (Supplementary Fig. 5, Methods). Interestingly, acute whisker stimulation also leads to a $\sim 30\%$ average increase in shaft sGluA1 intensity (Fig. 3c, Supplementary Fig. 3e, f). These findings indicate sensory experience can drive increases in surface AMPARs in both dendritic spines and shafts.

We next examined whether whisker stimulation induced changes in spine sGluA1 are dendrite specific by grouping spines belonging to the same dendrite. One hour after whisker stimulation, spine sGluA1 increased more than 30% in 11 out of 52 dendrites (Fig. 3f, g). Across these 11 dendrites, spine sGluA1 increased approximately two-fold by an average of 202.2%. In control animals, the average spine sGluA1 in all 38 dendrites remained unchanged. These data indicate that only a subpopulation of dendrites ($\sim$ 20%) respond to sensory stimuli by modifying their surface AMPARs and are consistent with previous findings that layer 2/3 excitatory neurons of sensory cortex show high stimulus selectivity[19-21]. Interestingly, these 11 dendrites are evenly distributed across animals. However, since we could not unambiguously assign every dendrite to a specific neuron in this data set, we were not able to group these 52 dendrites further and investigate potential differences between neurons or effects of dendritic branch order.

Acute whisker stimulation shows small effects on spine size and spine turnover

Previous imaging studies in cultured slices have shown that LTP induction leads to spine enlargement[22] and LTD induction leads to spine shrinkage[23], although Sdrulla and Linden found no association between LTD expression and dendritic spine shrinkage in cerebellar Purkinje cells in acute slices[24]. It has also been shown using electron microscopy that a 24-hour period of single whisker stimulation in adult mice results in a significant increase in the density of synapses in the corresponding cortical barrel[25]. Our imaging approach is unique in its ability to measure the temporal dynamics of surface AMPARs and the mechanisms of their regulation in real time. We examined spine structure intensity at 0, 1, 2, and 3 hours following 10 Hz whisker stimulation. Although there was a slight trend towards an increase in spine size, on average we did not detect a significant change in spine structure intensity following whisker stimulation when compared to control (Fig. 3a, e, Supplementary Fig. 3a, b). This result indicates that acute whisker stimulation for 1 hour does not have a large effect on spine size *in vivo*.

Dendritic spines are dynamic and may provide a structural basis for information storage, and spine turnover has been suggested to play a important role in synaptic plasticity[26]. Spine turnover has been characterized in response to chronic sensory deprivation and motor learning[27,28,29]. However, over this short period of time (3 hours after the end of whisker stimulation) we saw very little spine turnover in the apical dendrites of layer 2/3 neurons and the rate of this turnover was not significantly affected by whisker stimulation (Supplementary Fig. 4). Thus, for the remainder of this study we have focused on AMPAR dynamics in the preexisting stable spines during sensory manipulation.

Initial spine and shaft properties have effects on spine changes

Spines *in vivo* have heterogeneous size and AMPAR content, likely reflecting differences in prior activity, and these differing basal states may affect the manner in which individual spines respond to future experience[30]. Indeed, It has been shown that small spines are preferential sites for long-term synaptic potentiation in brain slices[22]. When we examined the correlation coefficient between the initial spine size and the changes in spine size at hour 1 following whisker stimulation, we found that there is a significant negative correlation (Supplementary Fig. 6a, $r = -0.2546$, $p < 0.001$), showing that small spines increase in size

more than large spines following whisker stimulation. We also observed a smaller but significant negative correlation between initial spine size and changes in spine sGluA1 at hour 1 following whisker stimulation (Supplementary Fig. 6b, $r = -0.1057$, $p = 0.012$), indicating that small spines increase in GluA1 content more than large spines following whisker stimulation. In contrast, we found no significant trend in changes in shaft sGluA1 between small and large spines (Supplementary Fig. 6c, $r = 0.0685$, $p > 0.05$). Although there is a trend of positive correlation between changes in spine sGluA1 and initial spine sGluA1 or initial shaft sGluA1 following whisker stimulation, it is not statistically significant (Supplementary Fig. 6d, e). Interestingly, a significant positive correlation was detected between initial shaft sGluA1 and changes in shaft sGluA1 following whisker stimulation (Supplementary Fig. 6f, $r = 0.1608$, $p < 0.001$). All together, these results suggest that the initial spine properties can affect spine changes following whisker stimulation.

Changes in spine sGluA1 are positively correlated with spine size and shaft sGluA1

The interesting relationships among spine size, spine sGluA1 and shaft sGluA1 prompted us to investigate the correlations among changes in these three parameters following whisker stimulation. Although we did not detect a significant stimulation-evoked increase in spine size on average, we observed a significant positive correlation between changes in spine sGluA1 intensity and changes in spine size at hour 1 (Fig. 4a, $r = 0.44$). A one-sample t test reveals that the spine population in stimulated animals has a mean that lies significantly above the y = x line. These results indicate that while changes in spine size and sGluA1 content are correlated, whisker stimulation produces a much larger increase in spine sGluA1 than in spine size, suggesting an increase in density of sGluA1 in spines after whisker stimulation. This is consistent with our result that the total average spine sGluA1 increases $\sim 30\%$ while the total average spine size only shows a 6% increase following whisker stimulation (Fig. 2a, b). Next, when we examined changes in spine size in spines that showed a > 30% increase in GluA1 content we observed a 24% increase in spine size compared to a 93.5% increase in GluA1 content seen in these spines (Supplementary Fig. 7). Interestingly, the change in GluA1 content and spine size were not well correlated in this population of spines ($r = 0.12$) suggesting that increases in GluA1 content and spine size can be uncoupled. In addition, we found there is a significant positive correlation between changes in spine sGluA1 intensity and adjacent shaft sGluA1 intensity in stimulated animals (Fig. 4b, $r = 0.67$). In contrast, changes in shaft sGluA1 and spine size are not correlated (Fig. 4c, $r = 0.03$). Together, these findings indicate that acute whisker stimulation induces a coordinated increase in spine sGluA1 and shaft sGluA1 while changes in spine size can be uncoupled from sGluA1 changes.

Ex vivo studies have demonstrated clustered synaptic potentiation following sensory deprivation by whisker trimming [7] and *in vivo* imaging has shown clustered spine turnover induced by motor learning [27]. We see that increases in spine sGluA1 occur on a subset of dendrites after acute whisker stimulation and thus these increases were generally colocalized along dendritic segments. To address the distribution of sGluA1 increases on a finer spatial scale, we plotted the change in spine sGluA1 for each spine versus its nearest neighbor at 1 hour we found a significant positive correlation between neighboring spines ($r = 0.52$, $p <$

0.001). In addition, when grouped spines which change in the same direction with their neighbors (Fig. 4d, x > 130% and y > 130%, x < 70% and y < 70%, Group 1) and spines which change in the opposite direction with their neighbors (Fig 4d, x > 130% and y < 70%, x < 70% and y > 130%, Group 2), we found that the number of neighboring spines changing in the same direction is significantly more than chance (Fig. 4e), while the number of neighboring spines changing in the opposite direction is significantly less than chance (Fig. 4f). These results demonstrate that spine sGluA1 in neighboring spines change cooperatively following whisker stimulation. No such significant positive trend was found between neighboring spines in control animals (Fig. 4g).

Increase in spine sGluA1 is NMDA receptor dependent and is stable for 48 hours

One of the hallmarks of the most common form of LTP is that its induction is dependent on the activation of NMDA receptors[1-3]. To test whether the whisker stimulated increases in spine sGluA1 were NMDA receptor dependent, we injected the NMDA receptor antagonist CPP (3-(2-Carboxypiperazin-4-yl)-propyl-1-phosphonic acid) at 10 mg/kg, 30–45 minutes prior to whisker stimulation[6]. Remarkably, CPP application completely blocked the increase in both spine and shaft sGluA1 following whisker stimulation (Fig. 5a–d) indicating that this form of AMPAR plasticity is an NMDA-receptor dependent process.

Another characteristic of LTP is that it is long lasting and is maintained for several hours *in vitro* measured using extracellular field recordings and for several days or even months *in vivo* as measured using chronic field recordings[1-3]. To determine if the increase in spine sGluA1 is long lasting, we imaged neurons for up to two days after whisker stimulation. We found that the 30% increase in spine sGluA1 following whisker stimulation is maintained for at least 48 hours (Fig. 6a, c), while changes in spine size were on average, small, and not significant (Fig. 6b). Interestingly, the initial 30% increase at hour 1 in shaft sGluA1 following whisker stimulation (Fig. 2c) decreases to 10% by hour 6, and returns to un-stimulated levels by 48 hours (Fig. 6d). Furthermore, the initial correlation between changes in spine sGluA1 and shaft sGluA1 becomes weaker over time, and no significant correlation remains at hour 48 (Supplementary Fig. 8). These results suggest shaft sGulA1 insertion and spine sGluA1 incorporation are two related but distinct events such that initial extrasynaptic (shaft) insertion of sGluA1 may supply GluA1 for spine incorporation, but after stabilization of the increased spine sGluA1, the levels of shaft sGluA1 decline. Together, these results demonstrate that acute whisker stimulation leads to a NMDA receptor-dependent LTP-like phenomenon that results in long-lasting spine surface incorporation of GluA1.

Discussion

Our study visualizes AMPARs in vivo in live animals and the real time dynamic expression of AMPARs in response to sensory stimulation. We demonstrate that acute whisker stimulation drives increases in surface GluA1 in both spines and dendritic shafts *in vivo*. Interestingly, only a subset of dendrites in the stimulated barrel column respond to sensory stimuli by modifying their surface GluA1 levels. The initial spine properties can affect future experience-dependent changes in spines. Specifically, small spines increase more in size and sGluA1 content than large spines following whisker stimulation. Absolute changes

and percent changes (relative changes) of sGluA1 are two different ways of quantifying spine changes following stimulation and we have used both methods in this manuscript to characterize the properties of synapse dynamics. However, percent changes may be more relevant physiologically since synaptic plasticity, such as LTP, is usually quantified as percent changes from baseline synaptic transmission. Increases in spine sGluA1 following whisker stimulation are well coordinated with and distinct from changes in shaft sGluA1. This shaft sGluA1 may serve as a pool of extrasynaptic AMPARs utilized for synaptic recruitment after stimulation. Furthermore, sGluA1 in neighboring spines tends to change in the same direction following whisker stimulation, suggesting neighboring spines a cooperatively increase their AMPARs content. Finally, the increase in spine sGluA1 evoked by whisker stimulation is NMDA receptor dependent and long lasting, indicating that *in vivo* whisker stimulation may induce an LTP like phenomenon in layer 2/3 pyramidal neurons similar to what has recently been shown by *in vivo* electrophysiological techniques[31].

In most previous studies, spine structural dynamics have been used as a measure of synaptic plasticity. However, we see no significant difference in spine turnover between stimulated and control animals during the same time frame in which we see significant changes in sGluA1. These results indicate that investigating spine turnover in isolation might miss key plasticity events occurring within already existing spines. Although the level of spine AMPARs does not directly measure synaptic strength, spine AMPAR content is a well known strong correlate of synaptic strength[1-3] and it has been established that synaptic connections can be strengthened or weakened by adding or removing synaptic AMPA receptors[1-3]. AMPA receptor imaging allows us to reveal additional information about the dynamic plasticity that is occurring in spines in addition to investigating spine dynamics and spine size changes. In most spine imaging studies the number of spines that change in response to activity is quite small. In contrast, our data shows that plasticity at preexisting spines is much more widespread and the ability to image receptors *in vivo* opens up a totally new way to image plasticity. Our study is the first to examine AMPARs *in vivo* allowing us to directly observe, in real time, AMPAR dynamics in response to sensory experience. Future experiments examining AMPAR dynamics during plasticity in other cortical regions and in mouse lines in which various key synaptic proteins, such as PSD-95, SAP-97, and PICK1 have been deleted or altered will help identify the essential regulators of AMPAR trafficking *in vivo* and elucidate the molecular mechanisms underlying long term synaptic plasticity in the brain.

Methods

All experimental protocols were conducted according to the National Institutes of Health guidelines for animal research and were approved by the Animal Care and Use Committee at Johns Hopkins University School of Medicine.

In utero electroporation

Layer 2/3 progenitor cells were transfected by *in utero* electroporation of E15 embryos from timed pregnant C57BL/6J mice (Charles River) as previously described[8]. Approximately, 0.2 μl of DNA solution containing fast green as a marker was pressure injected into the

lateral ventricle of each embryo through a pulled-glass pipette. Five pulses of 35 V (50 ms on, 950 ms off @1 Hz) were delivered, targeting the barrel cortex, using 5 mm tweezer electrodes connected to a square wave electroporator (CUY21, π Protech). SEP-GluA1, myc-GluA2 and Dsred2 were used for *in utero* electroporation at a 4:4:1 ratio. GluA2 was included in an attempt to approximate the natural GluA1/GluA2 ratio in transfected cells.

Craniotomy

Pups born after *in utero* electroporation (males and females) were implanted with a cranial window overlaying the barrel cortex region at the age of 10–12 weeks as previously described[10]. The antibiotics sulfamethoxazole (1 mg/ml) and trimethoprim (0.2 mg/ml) were chronically administered in the drinking water and the animals were housed individually after surgery.

Whisker stimulation

All whiskers were kept intact for all mice. A single whisker (B2, C2, or D2) was deflected at 10 Hz for 1 hour and images were taken in the corresponding barrel column in the contralateral hemisphere.

Intrinsic optical signal imaging

Two to three weeks after the cranial window surgery, intrinsic optical signal imaging was performed as described previously[12]. Mice were anesthetized and maintained on 0.5% isofluorane supplemented by xylazine (13 mg/kg). Optical images of the barrel cortex were acquired at 30 Hz using a CCD camera (Sony XC-ST70) under red LED light (630 nm) with a $2.5 \times /0.075$ NA Plan Neofluar Zeiss objective. Images were first converted to 32-bit depth to display results with high precision, and then the multi-frame image stacks were averaged across 30 trials. Next, images were collapsed across time, separately averaging 15 baseline and 15 response frames. Finally, these two images were Gaussian filtered ($\sigma = 10$ μm) and baseline subtracted.

Two-photon imaging

In vivo images were acquired under isoflurane anesthesia (0.5% vol isoflurane/vol O_2) using a custom-built, two-photon laser-scanning microscope controlled by ScanImage written in MATLAB[32]. Apical dendrites of layer 2/3 pyramidal neurons of the mouse barrel cortex were imaged using a $20 \times /1.0$ NA water immersion objective lens (Zeiss). SEP-GluA1 and dsRed2 were excited at 910 nm with a Ti:sapphire laser (Coherent) with ~ 100 mW power delivered to the back-aperture of the objective. Green and red fluorescence signals were separated by a set of dichroic mirrors (MOM system, Sutter Instrument) and filters (ET525/50m for green channel, ET605/70m for red channel, Chroma). Images stacks were acquired at 1024×1024 pixels with a voxel size of 0.18 μm in x and y with a z-step of 1 μm. Representative images shown in figures were median filtered, up-scaled and contrast enhanced.

Spine analysis

All spine dynamics and intensity analysis were performed using custom written software in Igor Pro (WaveMetrics, Lake Oswego, Oregon). Documentation for the software can be found at http://robertcudmore.org/.

Spine dynamics

Spines within each time-point were visually identified and manually marked as a 3D point at their tip using the raw image stacks from the structural dsRed2 channel. Each dendrite ($\sim$ 100 µm) was traced to produce a dendritic backbone and radius using a modified version of the Simple Neurite Tracer Plugin in FIJI[33]. The same dendritic tracing and spine markings were used for both spine turnover and intensity analysis. Manually marked spines were automatically connected to the dendritic backbone by following the brightest linear path. This connection point gives each spine a distance (in µm) along the dendritic backbone from a manually identified fiduciary point (common to all image stacks) and is used to semi-automatically identify corresponding spines from one image stack to the next. Finally, the connection point of each spine to the dendritic backbone and the correspondence of spines between time-points was visually verified and manually edited for errors. For a spine to be included in the final analysis, it must protrude from the dendritic backbone by more than 4 pixels (> 0.72 µm) and be primarily parallel to the imaging plane. Spines that are present from one time-point to the next are categorized as 'persistent', spines that are present in a given time-point but absent in the previous are categorized as 'added' and spines that are present in a given time-point but not in the next are categorized as 'subtracted'.

Intensity analysis

The same dendritic tracing and spine markings were used for spine turnover and intensity analysis. Only spines that could be visually identified in all time-points were included in the final intensity analysis. Each spine was assigned three different non-overlapping regions of interest (ROIs): $spine_{ROI}$, $shaft_{ROI}$ and $background_{ROI}$. The $spine_{ROI}$ enclosed the spine head and did not include pixels within the radius of the dendritic backbone. The $shaft_{ROI}$ was constructed from the backbone line and radius of the dendrite, centered on each spine and expanded along the dendrite to match the number of pixels in the $spine_{ROI}$. The $background_{ROI}$ (same shape and number of pixels as the $spine_{ROI}$) was translated in x/y to a nearby region of the image that was representative of the background fluorescence.

Each $spine_{ROI}$ is defined by a width (1 µm) and all ROIs extend in 3D up and down from the best imaging plane ($\pm$ 1 plane). The intensity analysis was parameterized to check that our results remained consistent. Briefly, we varied both the spine width (0.8–1.2 µm) and the ROIs $\pm$ plane (0–3 planes) and obtained similar results.

To measure the spine intensity for the SEP-GluA1 channel, the same three ROIs for each spine were applied to the green/SEP-GluA1 channel. The $spine_{ROI}$ and $backbone_{ROI}$ were in the same position while the $background_{ROI}$ was again translated in x/y to minimize the background intensity in the green/SEP-GluA1 channel. All spine and shaft intensity measures were normalized to the shaft of the red channel as follows:

$$Spine\ Structure\ Intensity = (\sum Spine_{ROI,dsRed2} - \sum Background_{ROI,dsRed2}) / \sum Shaft_{ROI,dsRed2}$$

$$Spine\ sGluA1\ Intensity = (\sum Spine_{ROI,GluA1} - \sum Background_{ROI,GluA1}) / \sum Shaft_{ROI,dsRed2}$$

$$Shaft\ sGluA1\ Intensity = (\sum Shaft_{ROI,dsRed2} - \sum Background_{ROI,dsRed2}) / \sum Shaft_{ROI,dsRed2}$$

Here, the dsRed2 and GluA1 subscripts refer to the intensities obtained from the red/dsRed2 and green/SEP-GluA1 channels respectively.

We have carefully examined the z-planes above and below the spine and shaft ROIs to confirm that our intensity values are not contaminated by signal from spines protruding out of the imaging plane.

Categorizing changes in spine intensity

To group spines into up, down, and same categories we used the SD of percent change in control at hour 1 as a threshold (30% for spine sGluA1, Fig. 3d, g and Fig. 4d).

Monte-Carlo simulations

We tested if the number of spines observed in group 1 (upper right or lower left regions) of Fig. 4e occurred by chance using a Monte-Carlo method by randomly shuffling each spines nearest neighbor spine GluA1 intensity and counting the number of spines in group 1. A p value was calculated as $(n + 1)/(r + 1)$, where n is the number of shuffles with the number of spines in group 1 greater than the number we observed and r is the number of shuffles (10,000). The same Monte-Carlo method was used for Fig. 4f where n is the number of shuffles with the number of spines in group 2 (upper left or lower right regions) less than the number we observed and r is the number of shuffles (10,000).

Statistical analysis

Data distribution was assumed to be normal but was not formally tested. No statistical methods were used to predetermine sample sizes, but our sample sizes are similar to those generally employed in the field. When possible we used Monte-Carlo shuffling or the non-parametric Mann-Whitney test (noted in Figure legends). Otherwise, we assumed the data points have a normal distribution and used ANOVA or t-test. All the tests were two-sided. Data collection and analysis were not performed blind to the conditions of the experiments. Animals were randomly assigned to control or whisker stimulation groups if they have detectable signal in the barrel cortex for two photon imaging two weeks after surgery.

Supplementary Material

Refer to Web version on PubMed Central for supplementary material.

Acknowledgments

References

1. Huganir RL, Nicoll RA. AMPARs and Synaptic Plasticity: The Last 25 Years. Neuron. 2013; 80:704–717. [PubMed: 24183021]

2. Lee HK, Kirkwood A. AMPA receptor regulation during synaptic plasticity in hippocampus and neocortex. Seminars in cell & developmental biology. 2011; 22:514–520. [PubMed: 21856433]

3. Luscher C, Malenka RC. NMDA receptor-dependent long-term potentiation and long-term depression (LTP/LTD). Cold Spring Harbor perspectives in biology. 2012; 4

4. Zuo Y, Yang G, Kwon E, Gan WB. Long-term sensory deprivation prevents dendritic spine loss in primary somatosensory cortex. Nature. 2005; 436:261–265. [PubMed: 16015331]

5. Holtmaat A, Wilbrecht L, Knott GW, Welker E, Svoboda K. Experience-dependent and cell-type-specific spine growth in the neocortex. Nature. 2006; 441:979–983. [PubMed: 16791195]

6. Clem RL, Celikel T, Barth AL. Ongoing in vivo experience triggers synaptic metaplasticity in the neocortex. Science. 2008; 319:101–104. [PubMed: 18174444]

7. Makino H, Malinow R. Compartmentalized versus Global Synaptic Plasticity on Dendrites Controlled by Experience. Neuron. 2011; 72:1001–1011. [PubMed: 22196335]

8. Saito T, Nakatsuji N. Efficient gene transfer into the embryonic mouse brain using in vivo electroporation. Developmental biology. 2001; 240:237–246. [PubMed: 11784059]

9. Petersen CC. The functional organization of the barrel cortex. Neuron. 2007; 56:339–355. [PubMed: 17964250]

10. Holtmaat A, et al. Long-term, high-resolution imaging in the mouse neocortex through a chronic cranial window. Nature protocols. 2009; 4:1128–1144. [PubMed: 19617885]

11. Xu HT, Pan F, Yang G, Gan WB. Choice of cranial window type for in vivo imaging affects dendritic spine turnover in the cortex. Nature neuroscience. 2007; 10:549–551. [PubMed: 17417634]

12. Harrison TC, Sigler A, Murphy TH. Simple and cost-effective hardware and software for functional brain mapping using intrinsic optical signal imaging. Journal of neuroscience methods. 2009; 182:211–218. [PubMed: 19559049]

13. Kopec CD, Real E, Kessels HW, Malinow R. GluR1 links structural and functional plasticity at excitatory synapses. J Neurosci. 2007; 27:13706–13718. [PubMed: 18077682]

14. Noguchi J, et al. In vivo two-photon uncaging of glutamate revealing the structure–function relationships of dendritic spines in the neocortex of adult mice. The Journal of Physiology. 2011; 589:2447–2457. [PubMed: 21486811]

15. O'Brien RJ, et al. Activity-dependent modulation of synaptic AMPA receptor accumulation. Neuron. 1998; 21:1067–1078. [PubMed: 9856462]

16. Mammen AL, Huganir RL, O'Brien RJ. Redistribution and stabilization of cell surface glutamate receptors during synapse formation. J Neurosci. 1997; 17:7351–7358. [PubMed: 9295381]

17. Clem RL, Barth A. Pathway-specific trafficking of native AMPARs by in vivo experience. Neuron. 2006; 49:663–670. [PubMed: 16504942]

18. Takahashi T, Svoboda K, Malinow R. Experience strengthening transmission by driving AMPA receptors into synapses. Science. 2003; 299:1585–1588. [PubMed: 12624270]

19. Petersen CC, Crochet S. Synaptic computation and sensory processing in neocortical layer 2/3. Neuron. 2013; 78:28–48. [PubMed: 23583106]

20. Crochet S, Poulet JF, Kremer Y, Petersen CC. Synaptic mechanisms underlying sparse coding of active touch. Neuron. 2011; 69:1160–1175. [PubMed: 21435560]

21. O'Connor DH, Peron SP, Huber D, Svoboda K. Neural activity in barrel cortex underlying vibrissa-based object localization in mice. Neuron. 2010; 67:1048–1061. [PubMed: 20869600]

22. Matsuzaki M, Honkura N, Ellis-Davies GC, Kasai H. Structural basis of long-term potentiation in single dendritic spines. Nature. 2004; 429:761–766. [PubMed: 15190253]

23. Nagerl UV, Eberhorn N, Cambridge SB, Bonhoeffer T. Bidirectional activity-dependent morphological plasticity in hippocampal neurons. Neuron. 2004; 44:759–767. [PubMed: 15572108]

24. Sdrulla AD, Linden DJ. Double dissociation between long-term depression and dendritic spine morphology in cerebellar Purkinje cells. Nature neuroscience. 2007; 10:546–548. [PubMed: 17435753]

25. Knott GW, Quairiaux C, Genoud C, Welker E. Formation of dendritic spines with GABAergic synapses induced by whisker stimulation in adult mice. Neuron. 2002; 34:265–273. [PubMed: 11970868]

26. Bhatt DH, Zhang S, Gan WB. Dendritic spine dynamics. Annual review of physiology. 2009; 71:261–282.

27. Fu M, Yu X, Lu J, Zuo Y. Repetitive motor learning induces coordinated formation of clustered dendritic spines in vivo. Nature. 2012; 483:92–95. [PubMed: 22343892]

28. Trachtenberg JT, et al. Long-term in vivo imaging of experience-dependent synaptic plasticity in adult cortex. Nature. 2002; 420:788–794. [PubMed: 12490942]

29. Yang G, Chang PC, Bekker A, Blanck TJ, Gan WB. Transient effects of anesthetics on dendritic spines and filopodia in the living mouse cortex. Anesthesiology. 2011; 115:718–726. [PubMed: 21768874]

30. Perez-Otano I, Ehlers MD. Homeostatic plasticity and NMDA receptor trafficking. Trends Neurosci. 2005; 28:229–238. [PubMed: 15866197]

31. Gambino F, et al. Sensory-evoked LTP driven by dendritic plateau potentials in vivo. Nature. 2014

32. Pologruto TA, Sabatini BL, Svoboda K. ScanImage: flexible software for operating laser scanning microscopes. Biomedical engineering online. 2003; 2:13. [PubMed: 12801419]

33. Longair MH, Baker DA, Armstrong JD. Simple Neurite Tracer: open source software for reconstruction, visualization and analysis of neuronal processes. Bioinformatics. 2011; 27:2453–2454. [PubMed: 21727141]
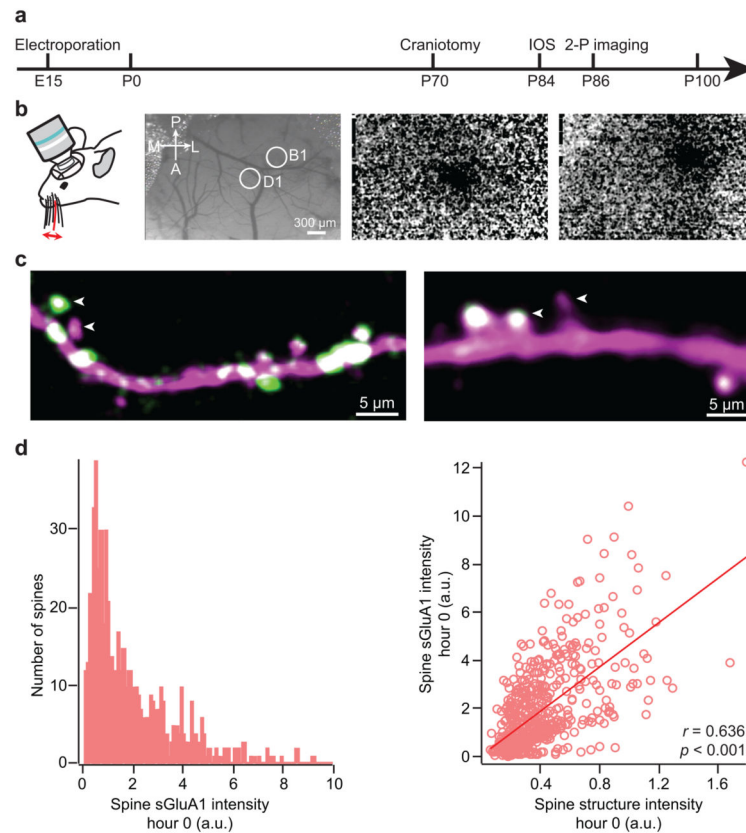
Figure 1. Expression of SEP-GluA1 in layer 2/3 barrel cortex neurons *in vivo*
a, Time line of experimental design. IOS = intrinsic optical signal imaging. **b,** Intrinsic optical signal imaging. Cortical surface blood vessels can be imaged with green light (left). 10 Hz deflection of the D1 (center) or B1 (right) whisker evokes a localized change in reflected red light resulting from the coupling of blood flow to neural activity. **c.** Representative images showing expression of dsRed2 (magenta) and SEP-GluA1 (green). Note the different SEP-GluA1 level in neighboring spines (arrowheads). **d,** Histogram of spine sGluA1 intensity before whisker stimulation at hour 0 (left). Correlation between spine sGluA1 and spine size before whisker stimulation at hour 0 (right). *r*, Pearson's linear correlation coefficient, *p* value is from Monte-Carlo shuffling.
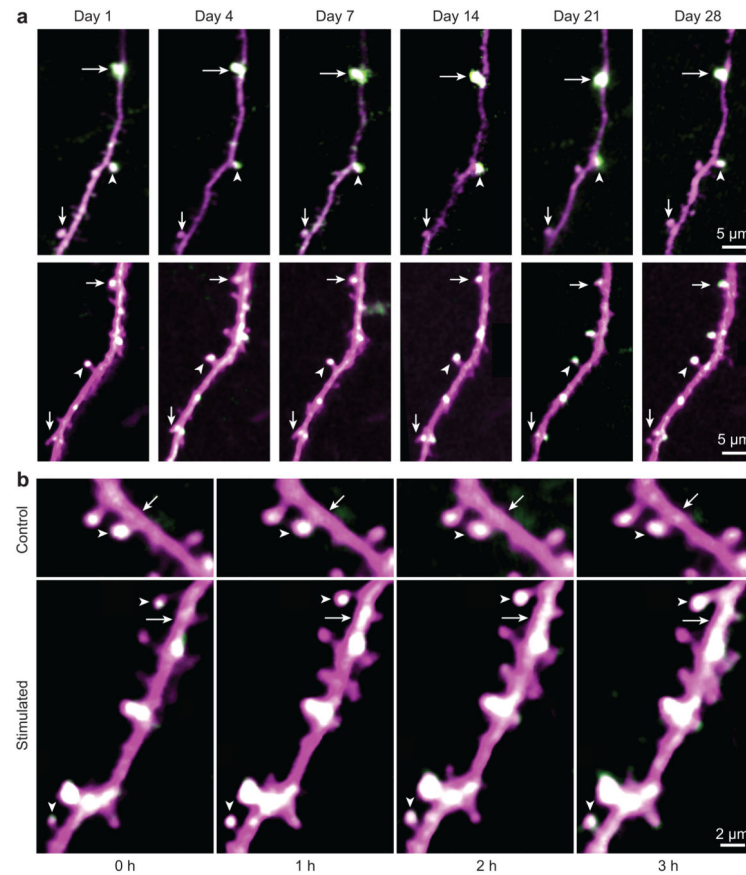
Figure 2. Acute whisker stimulation leads to an increase in spine sGluA1 *in vivo* in apical dendrites of layer 2/3 neurons in the barrel cortex
a, Long-term stable expression of SEP-GluA1 and dsRed2. Same spines were marked with arrows and arrowheads in different imaging sessions. **b,** Representative time-lapse *in vivo* 2-photon images of layer 2/3 pyramidal cell apical tuft dendrites taken with no whisker stimulation (Control) or before (Stimulated, hour 0) and after 1-hour-long acute whisker stimulation (Stimulated, hour 1, 2, and 3). Arrowheads mark spines and arrows mark dendritic shafts (SEP-GluA1 in green, dsRed2 in magenta, overlap in white). Images are single plane median filtered images that were up-scaled and contrast enhanced.
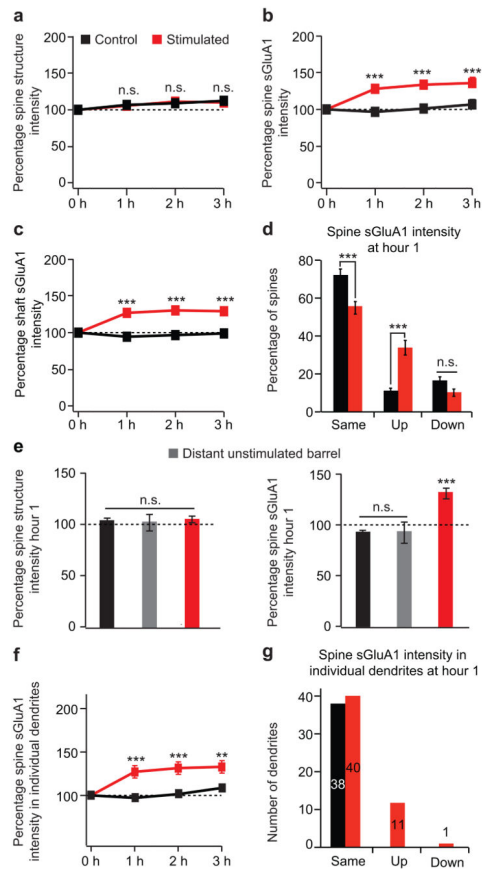
Figure 3. Acute whisker stimulation leads to an increase in spine sGluA1 and shaft sGluA1, but has little effect on spine size

a, Spine structure intensity (dsRed2 signal) at hour 0, 1, 2, and 3 in control and stimulated animals. **b,** Spine sGluA1 intensity (SEP-GluA1 signal) in control and stimulated animals. **c,** Shaft sGluA1 intensity in control and stimulated animals. **d,** Categorization of spine sGluA1 responses at hour 1, same (> 70% and < 130%), up (130%), and down (70%). **e,** Changes in spine structure intensity (left) and in spine sGluA1 intensity (right) at hour 1 in distant unstimulated barrels. **f,** Average sGluA1 intensity in spines belonging to the same dendrites in control and stimulated animals. **g,** Categorization of dendritic responses at hour 1 into the same, up, and down categories (same criterion as panel d). 585 spines, 52 dendrites in 6 stimulated animals; 493 spines, 38 dendrites in 5 control animals. 40 spines, 6 dendrites in 2 animals (distant unstimulated barrel in e). ***$p < 0.001$, **$p < 0.01$, two-way analysis of variance (ANOVA) with Bonferroni posttests. Error bars = s.e.m.
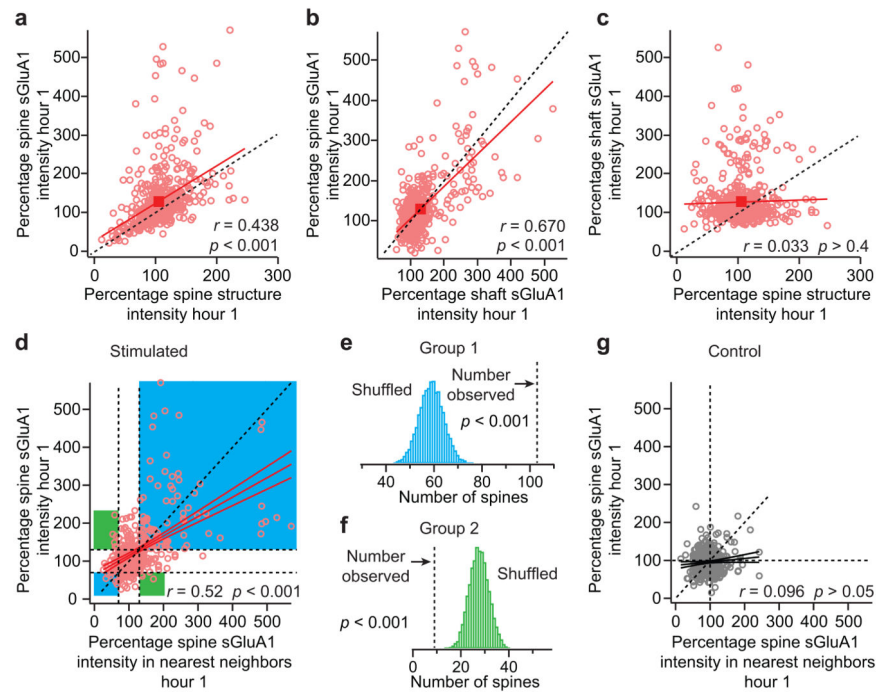
Figure 4. Changes in spine sGluA1 are positively correlated with shaft sGluA1 and spine size following whisker stimulation and neighboring spines cooperatively increase their spine sGluA1
a, Correlation between spine sGluA1 and spine structure intensity at hour 1 in stimulated animals. **b,** Correlation between spine sGluA1 and shaft sGluA1 at hour 1 in stimulated animals. **c,** Correlation between shaft sGluA1 and spine structure intensity at hour 1 in stimulated animals. **d,** Changes in spine sGluA1 in neighboring spines at hour 1 in stimulated animals with linear fits ($r = 0.5206$, $p < 0.001$). Spine sGluA1 change in the same direction in neighboring spines were highlighted in light blue (x > 130% and y > 130%, x < 70% and y < 70%, Group 1), spine sGluA1 change in the opposite direction in neighboring spines were highlighted in green (x > 130% and y < 70%, x < 70% and y > 130%, Group 2). Dotted vertical line, left = 70%, right = 130%. Dotted horizontal line, upper = 130%, lower = 70%. **e,** Histogram of 10,000 random shuffles of the number of spines that change in the same direction with their neighboring spines in spine sGluA1. Dotted vertical line, the observed number of spines (103, Group 1 in panel d). Monte-Carlo p value is calculated by summing the tail of the shuffled histogram (Methods). **f,** Histogram of 10,000 random shuffles of the number of spines that change in the opposite direction with their neighboring spines in spine sGluA1. Dotted vertical line, the observed number of spines (9, Group 2 in panel d). Monte-Carlo p value is calculated by summing the tail of the shuffled histogram (Methods). **g,** Changes in spine sGluA1 in neighboring spines at hour 1 in control animals with linear fits ($r = 0.096$, $p = 0.06$). r, Pearson's linear correlation coefficient. p, Pearson's correlation t test.
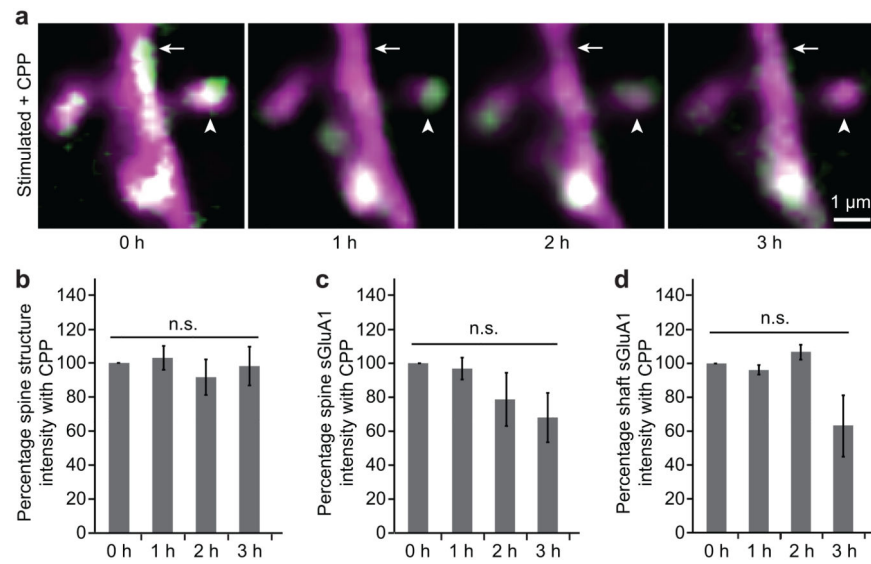
Figure 5. Increase in spine sGluA1 following whisker stimulation is NMDA receptor dependent
a, Representative images of dendrites taken before (0 hour) and after (hour 1, 2, 3) acute whisker stimulation in animals with CPP treatment. Arrowheads mark spines and arrows mark dendritic shafts (SEP-GluA1 in green, dsRed2 in magenta, overlap in white). **b,** Spine structure intensity following whisker stimulation with CPP treatment. **c,** Spine sGluA1 intensity following whisker stimulation with CPP treatment. **d,** Shaft sGluA1 intensity following whisker stimulation with CPP treatment. 30 spines, 5 dendrites in 2 animals for CPP treatments. Two-way ANOVA with Bonferroni posttests. Error bars = s.e.m.
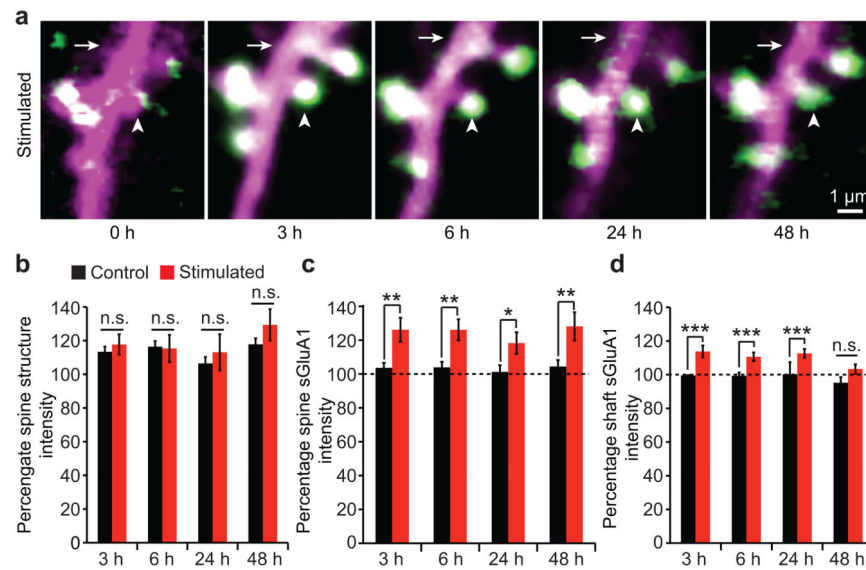
Figure 6. Increase in spine sGluA1 following whisker stimulation is stable for 48 hours, while increase in shaft sGluA1 declines over time

a, Representative images of dendrites taken at hour 3, 6, 24, and 48 following acute whisker stimulation. Arrowheads mark spines and arrows mark dendritic shafts (SEP-GluA1 in green, dsRed2 in magenta, overlap in white). **b,** Spine structure intensity at hour 3, 6, 24, and 48 in control and stimulated animals. **c,** Spine sGluA1 intensity in control and stimulated animals. **d,** Shaft sGluA1 intensity in control and stimulated animals. 105 spines, 13 dendrites in 3 stimulated animals, 142 spines, and 16 dendrites in 3 control animals. ***$p < 0.001$, **$p < 0.01$, *$p < 0.05$, two-way ANOVA with Bonferroni posttests. Error bars = s.e.m.